TOXICOLOGICAL SCIENCES **106(2)**, 556–569 (2008)
doi:10.1093/toxsci/kfn198
Advance Access publication September 16, 2008

Global Liver Proteomics of Rats Exposed for 5 Days to Phenobarbital Identifies Changes Associated with Cancer and with CYP Metabolism

Mary B. Dail,*,† L. Allen Shack,† Janice E. Chambers,*,†,[1,2] and Shane C. Burgess†,‡,§,¶,[2]

*Center for Environmental Health Sciences, College of Veterinary Medicine; †Department of Basic Sciences, College of Veterinary Medicine; ‡Mississippi Agriculture and Forestry Experiment Station; §Institute for Digital Biology; and ¶Life Sciences and Biotechnology Institute, Mississippi State University, Mississippi State, Mississippi 39762

Received June 20, 2008; accepted September 10, 2008

A global proteomics approach was applied to model the hepatic response elicited by the toxicologically well-characterized xenobiotic phenobarbital (PB), a prototypical inducer of hepatic xenobiotic metabolizing enzymes and a well-known nongenotoxic liver carcinogen in rats. Differential detergent fractionation two-dimensional liquid chromatography electrospray ionization tandem mass spectrometry and systems biology modeling were used to identify alterations in toxicologically relevant hepatic molecular functions and biological processes in the livers of rats following a 5-day exposure to PB at 80 mg/kg/day or a vehicle control. Of the 3342 proteins identified, expression of 121 (3.6% of the total proteins) was significantly increased and 127 (3.8%) significantly decreased in the PB group compared to controls. The greatest increase was seen for cytochrome P450 (CYP) 2B2 (167-fold). All proteins with statistically significant differences from control were then analyzed using both Gene Ontology (GO) and Ingenuity Pathways Analysis (IPA, 5.0 IPA-Tox) for cellular location, function, network connectivity, and possible disease processes, especially as they relate to CYP-mediated metabolism and nongenotoxic carcinogenesis mechanisms. The GO results suggested that PB's mechanism of nongenotoxic carcinogenesis involves both increased xenobiotic metabolism, especially induction of the 2B subfamily of CYP enzymes, and increased cell cycle activity. Apoptosis, however, also increased, perhaps, as an attempt to counter the rising cancer threat. Of the IPA-mapped proteins, 41 have functions which are procarcinogenic and 14 anticarcinogenic according to the hypothesized nongenotoxic mechanism of imbalance between apoptosis and cellular proliferation. Twenty-two additional IPA nodes can be classified as procarcinogenic by the competing theory of increased metabolism resulting in the formation of reactive oxygen species. Since the systems biology modeling corresponded well to PB effects previously elucidated via more traditional methods, the global proteomic approach is proposed as a new screening methodology that can be incorporated into future toxicological studies.

Key Words: **cytochrome P450 induction; phenobarbital; global proteome; systems biology; cancer; DDF 2D LC ESI MS^2.**

Global proteomic techniques have not yet been utilized to their full potential in toxicology. These powerful techniques can identify and quantify proteins whose levels change in response to xenobiotic exposure and can relate these proteins to other proteins through a systems biology analysis. These techniques should thus have great applicability to identify early responses to xenobiotics and to characterize the cellular systems impacted. This approach was used to characterize the responses of the rat liver to a well-studied xenobiotic, phenobarbital (PB), to determine whether these methods identify protein networks associated with some of the known effects of this compound. PB is a prototypical inducer of hepatic xenobiotic metabolizing enzymes including the cytochromes P450 (CYPs) (Kakizaki *et al.*, 2003; Waxman and Azaroff, 1992), and its pleiotropic effects include hyperproliferation of the liver and endoplasmic reticulum, increased DNA synthesis, the repression of some genes yet induction of others, plus tumor promotion in animals (Corcos and Lagadic-Gossman, 2001). The mechanism of PB's promotion of hepatocarcinogenesis in monkeys (Biswas *et al.*, 2004) and rodents (Oliver and Roberts, 2002) is not genotoxic. Two main hypotheses exist to explain how PB increases rodent cancer risk. One multifaceted hypothesis proposes that decreases in apoptosis, intercellular communication, DNA repair time, and tumor suppressor gene function in concert with increased cell proliferation and other aberrant cellular activity all play roles in PB tumorigenesis (Kolaja *et al.*, 2000; Seidel *et al.*, 2006). The competing hypothesis is that increased metabolism, especially the barbiturate-type induction of the 2B subfamily of CYP enzymes, results in the formation of reactive oxygen species that, in turn, cause cancer (Dostalek *et al.*, 2007).

Because of its interesting effects on the liver, PB has been utilized in a number of liver gene expression studies using DNA microarrays (Gerhold *et al.*, 2001; Hamadeh *et al.*, 2002; Kier *et al.*, 2004; Kiyosawa *et al.*, 2004; Leone *et al.*, 2007; Nie *et al.*, 2006; Ueda *et al.*, 2002). These studies have shown that hundreds of genes are either induced or repressed by PB.

[1] To whom correspondence should be addressed at the Center for Environmental Health Sciences, College of Veterinary Medicine, Mississippi State University, 240 Wise Center Drive, PO Box 6100, Mississippi State, MS 39762-6100. Fax: (662) 325-1031. E-mail: chambers@cvm.msstate.edu.

[2] These authors jointly contributed to this work.

They include genes for metabolic enzymes from phases I, II, and III (Gerhold *et al*., 2001). The observed increases in mRNA levels are logical in light of PB's postulated mechanism of inducing proteins by increasing DNA transcription and mRNA stability (Parkinson, 2001; Waxman and Azaroff, 1992). However, transcriptional repression can also occur since some work suggests that the constitutive active/androstane receptor (CAR, NR1I3) functions both as an inducer and a repressor (Corcos and Lagadic-Gossman, 2001; Kakizaki *et al*., 2003).

There is also mounting evidence that the amount of mRNA formed may differ 20- to 30-fold from the proteins which are finally produced (Gygi *et al*., 1999), perhaps, because of the rapid degradation of mRNA transcripts as part of gene silencing (Guenther *et al*., 2007). In any case, several researchers have come to the conclusion that not all gene changes are predictive because the transcriptome is not the proteome and much can happen between transcription and the production of a functional protein (Desiere *et al*., 2004; Gygi *et al*., 1999; Kier *et al*., 2004; Kiyosawa *et al*., 2004). Proteomics identifies and quantifies proteins directly. Because of the complexity of the complete liver proteome, only a few one-dimensional bands or two-dimensional (2D) spots were originally identified (Amacher *et al*., 2005; Galeva *et al*., 2003; Nisar *et al*., 2004; Zgoda *et al*., 2006). More recently, coupling two-dimensional liquid chromatography electrospray ionization tandem mass spectrometry (2D LC ESI MS^2) to data analysis via the SEQUEST algorithm (Link *et al*., 1999) has made it practical to attempt global proteome determination. These advances have led to the global protein analysis of livers from both rats (Jiang *et al*., 2004) and humans (Chen *et al*., 2007).

Our group has developed differential detergent fractionation (DDF)-multidimensional protein identification technology (MudPIT) (McCarthy *et al*., 2005) which couples the DDF (commonly used prior to two-dimensional polyacrylamide gel electrophoresis) to 2D LC ESI MS^2 and MudPIT analysis. DDF has been shown to be a rapid, practical method of subfractionating eukaryotic cells to increase the visualization of the proteome (Ramsby *et al*., 1994). DDF uses a series of different detergents to sequentially extract cellular proteins. Analyzing all the DDF fractions with 2D LC ESI MS^2 and MudPIT has allowed us to collect comprehensive cellular proteomes that include a large proportion of membrane proteins (McCarthy *et al*., 2005). This method has been used successfully to model whole organs using proteomics (McCarthy *et al*., 2006a), and since each fraction is independently analyzed by 2D LC ESI MS^2, one can also track changes in a protein's cellular location that occur as a result of the experimental treatment.

In the present study, DDF 2D LC ESI MS^2 was utilized to examine the effects of 5-day PB exposure on the rat liver proteome. This was done by comparing the proteins from livers of controls and PB-treated rats using both Gene Ontology (GO) (Ashburner *et al*., 2000) and Ingenuity Pathways Analysis (IPA)'s new 5.0 IPA-Tox software (Ingenuity Systems, Inc., Redwood City, CA). To our knowledge, this is the first global proteomics analysis of liver from animals exposed to a xenobiotic. This method allowed us to test the two competing hypotheses of PB tumorigenesis and our results suggest that the effects of PB are mediated by increased cell cycle and metabolism but that apoptotic pathways are increased and not decreased. This approach has outstanding potential to identify changes early in an exposure to a toxicant that traditionally have only been observed as overt chronic toxicities, and may prove itself useful in the early identification of potential toxicities during drug discovery.

MATERIALS AND METHODS

Animal treatment and tissue processing. Adult male Sprague Dawley–derived rats were housed and fed as described previously (Dail *et al*., 2007). Three rats were treated ip with either saline (controls) or PB in saline at 80 mg/kg body weight/day (treated) for 5 days as described previously (Ma and Chambers, 1995). Following sacrifice on day 5, the livers were removed and stored at − 80°C as previously described (Dail *et al*., 2007).

Proteomics. Five 8-μm sections were taken from each of the three control and three experimental livers resulting in 15 sections from each group using a Triangle Biomedical Supply Co. Minotome Plus (Durham, NC) microtome. The sections were weighed prior to DDF as described (McCarthy *et al*., 2005). The resulting protein lysates were precipitated, resuspended, reduced, alkylated, digested, desalted, eluted, vacuum dried, resuspended, and normalized by weight (Buza and Burgess, 2007).

MS analysis was done by 2D LC ESI MS^2 using a Thermo Separations P4000 quaternary gradient pump LCQ Deca XP Plus (ThermoElectron Corporation, San Jose, CA) as described previously (McCarthy *et al*., 2005). Liquid chromatography was done by strong cation exchange (SCX) followed by reverse phase (RP) LC coupled directly in line with an ESI ion trap mass spectrometer which was configured as described previously (Buza and Burgess, 2007). Briefly, samples were loaded into an LC gradient ion 17 exchange system (Thermo Separations P4000 quaternary gradient pump coupled with a 0.32 × 100-mm BioBasic SCX column). A flow rate of 3 μl/min was used for both SCX and RP columns. A salt gradient was applied in steps of 0, 5, 10, 15, 20, 25, 30, 35, 40, 45,50, 57, 64, 71, 79, 90, 110, 300, and 700mM ammonium acetate in 5% acetonitrile (ACN) and 0.1% formic acid, and the resultant peptides were loaded directly into the sample loop of a 0.18 × 100-mm BioBasic C18 RPLC column (ThermoElectron). The RP gradient used 0.1% formic acid in ACN and increased the ACN concentration in a linear gradient from 5 to 30% in 30 min and then 30 to 65% in 9 min followed by 95% for 5 min and 5% for 15 min. The spectrum collection time was 59 min for every SCX step. The mass spectrometer was configured to optimize the duty cycle length with the quality of data acquired by alternating between a single full MS scan followed by three tandem MS scans on the three most intense precursor masses (as determined by Xcalibur software in real time) from the full scan. The collision energy was normalized to 35%. Dynamic mass exclusion windows were set at 2 min, and all the spectra were measured with an overall mass/charge (m/z) ratio range of 300–1700.

The rat nonredundant protein database was downloaded from the National Center for Biotechnology Institute (27 March 2006). Decoy database searching was done using a TurboSEQUEST cluster (Buza and Burgess, 2007; Elias and Gygi, 2007) to calculate the probability that a tandem MS match occurred by chance and, from these, the probability of the protein identification occurring by chance (MacCoss *et al*., 2002; Nesvizhskii *et al*., 2003). Only proteins that were identified with more than two peptides ≥ 6 amino acids long, each with a $p < 0.05$ (i.e., protein p value is 0.05^n, where n = number of peptides used to identify the protein), were used for further analysis. All protein identifications and their associated MS data have been submitted to the proteomics identifications database (PRIDE, http://www.ebi.ac.uk/pride; Experiment Accession 7970 and 7971). For nonisotopic quantitative analysis, we used

a variant of spectral counting with improved specificity as described (Bridges *et al*., 2007; Nanduri *et al*., 2005). Our ProteinMapper computer program (Allen *et al*., 2006) was used to estimate the proportions of proteins identified from different DDF fractions.

GO analysis. GO uses controlled vocabularies (ontologies) to describe gene products by their functions as cellular components (CCs) or their involvement in molecular functions (MFs) and biological processes (BPs). This is done in a species-independent manner and does not include functions involved in disease or affected by the environment. The GenInfo Identifier (GI) numbers of proteins showing a statistically significant change from control (Bonferroni correction value of < 0.05) were used to search AgBase (http://www.agbase.msstate.edu/) using GORetriever (Bridges *et al*., 2007; McCarthy *et al*., 2006b) for their corresponding UniProt and GO identification (ID) numbers (Ashburner *et al*., 2000). The GO ID numbers were then used to assign to each significantly changed protein the three organizing principles of GO: Cellular Component (CC), Molecular Function (MF), and Biological Process (BP). The GO ID number and assigned principles were then subjected to high-level analysis with GO Slim using the GOA whole proteome GOSlim set (McCarthy *et al*., 2007). The net regulatory effect was determined by subtracting the number of decreased proteins from the number of increased proteins in each GOSlim category. In addition to the high-level analysis, GO can be used to test specific hypotheses (McCarthy *et al*., 2007). In order to derive more toxicologically relevant information, a series of GO terms were selected based on previous works (Dostalek *et al*., 2007; Elrick *et al*., 2005; Kolaja *et al*., 2000; Seidel *et al*., 2006) which discussed PB's effect on xenobiotic metabolism and the possible mechanisms of its nongenotoxic hepatocarcinogenesis. The GO terms selected are shown in Table 1 along with their GO ID numbers. These were used to search the GO ID list of differentially expressed proteins derived from the AgBase search described above. Protein matches between the two groups were scored as agonistic (+ 1), antagonistic (− 1), or no effect (0) for carcinogenesis based on the function of the protein. These scores were then multiplied by the proportional increase or decrease (fold change) after PB exposure to derive a collective quantitative value that represents both the number of proteins associated with each hypothesis and the magnitude of their changes following PB exposure.

TABLE 1
GO ID Numbers Used to Generate a Hypothesis-Driven GO Model from the Protein List

GO ID Number	GO Term Description
GO 0000302	Response to reactive oxygen species
GO 0005243	Gap junction channel activity
GO 0006800	Oxygen and reactive oxygen species metabolic process
GO 0006805	Xenobiotic metabolic process
GO 0006915	Apoptosis
GO 0006916	Antiapoptosis
GO 0006917	Induction of apoptosis
GO 0006979	Response to oxidative stress
GO 0007049	Cell cycle
GO 0007154	Cell communication
GO 0008219	Cell death
GO 0008283	Cell proliferation
GO 0009410	Response to xenobiotic stimulus
GO 0019987	Negative regulation of antiapoptosis
GO 0033626	Activation of a receptor
GO 0042127	Regulation of cell proliferation
GO 0042178	Xenobiotic catabolic process
GO 0042908	Xenobiotic transport
GO 0042981	Regulation of apoptosis
GO 0043065	Positive regulation of apoptosis
GO 0043066	Negative regulation of apoptosis
GO 0045767	Regulation of antiapoptosis
GO 0045768	Positive regulation of antiapoptosis
GO 0050381	Unspecific monooxygenase activity
GO 0051726	Regulation of cell cycle

The IPA. Since PB does act in a species-specific manner to cause liver cancer through nongenotoxic mechanisms (Biswas *et al*., 2004; Oliver and Roberts, 2002), the IPA's 5.0 IPA-Tox software (Ingenuity Systems, Inc., http://www.ingenuity.com) was used as described by the manufacturer to model specific physiological processes affected by PB exposure. Drawing on published, peer-reviewed literature, IPA constructs networks of direct and indirect interactions between orthologous mammalian genes, proteins, and endogenous chemicals. These relationships include those which occur due to disease and/or environmental input. Each GI accession number was mapped to its corresponding gene object (node) in the Ingenuity Pathways Knowledge Base (IPKB). Human, mouse, and rat gene orthologs are represented as a single node based on the IPKB data available for the most highly evolved species. The magnitude and direction of changes were determined by forming a ratio between the gene objects showing statistically significant changes following PB exposure and their previous control levels. Since some values were zero, in order to avoid division by zero, 1 was added to all control and experimental values prior to ratio formation. In order to obtain as complete a picture as possible, the ratios for the increased and decreased gene objects were combined into one data set. The IPA program treated these ratios as fold changes, and gene objects with fold changes $\geq |2|$ were overlaid onto a global molecular network developed from information contained in the IPKB. Networks were then algorithmically generated based on their connectivity.

RESULTS AND DISCUSSION

Protein Identification

A total of 3342 proteins were identified ($p < 0.0025$). Of these, 121 (3.6%) proteins were present in amounts that were significantly greater in the livers of PB-treated rats compared to the livers of the saline controls. The livers of the PB-exposed rats also had 127 (3.8%) proteins whose levels were significantly less than their control amounts. The complete protein lists are in supplementary tables 1 and 2. The greatest increase was seen for CYP2B2 (167-fold), and eight of the 127 proteins with significantly increased expression were CYPs. The only cytochrome showing a significant decrease was cytochrome c. The constitutive active/androstane receptor (CAR/NR1I3) was also significantly increased (5-fold) compared with the control. Other proteins of toxicological interest that significantly increased included microsomal glutathione *S*-transferase (49-fold), UDP-glucuronosyltransferase 2B2 and 2B5 precursors (77- and 32-fold, respectively), epoxide hydrolase 1 (56-fold), and hypoxia-inducible factor 1 alpha (HIF1A) (26-fold).

GO Analysis

The GO analysis using the GOA Whole Proteome GOSlim Set identified changes in CC, MF, and BP that are shown in Figure 1. The changes seen in the GO CC ontology suggest that PB increased proteins associated with cell division and/or cell enlargement. Decreases in cytoplasm (cytosol plus organelles) and the intracellular component (cytosol plus organelles and the nucleus) may represent the hepatocellular hypertrophy

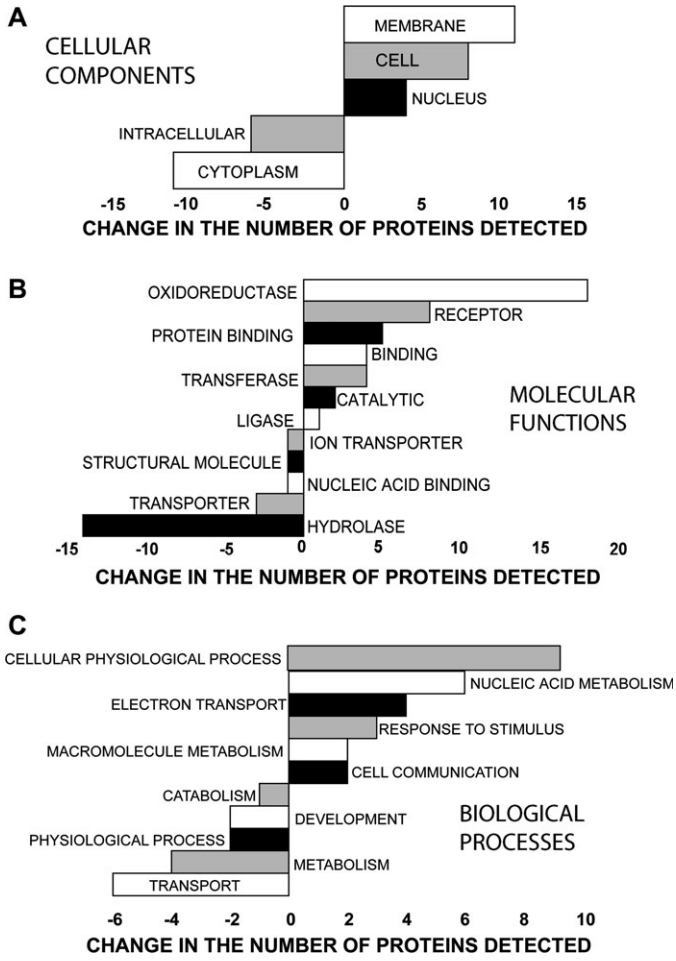

FIG. 1. GO modeling of the changes caused by PB in the proteins associated with (A) CC, (B) MF, and (C) BP.

commonly associated with PB (Parkinson, 2001). GO MF analysis shows that the greatest increase was in oxidoreductase activity, and since oxidoreductase activity is the primary enzymatic activity of CYPs and several CYPs are well known to be induced by PB, this lends credence to our analysis. The next three most increased MFs all involve the binding of proteins and molecules which are frequently associated with changes in cellular activity. The increases in transferase and catalytic activities could be another reflection of the increased CYP activity, and the increased ligase activity could indicate an increased need for DNA repair. Four of the five decreased MFs have the movement or assembly of biochemicals in common. GO MFs are grouped together into GO BPs. At this highest level of organization, many of the increased proteins are involved in BPs which lead to increases in DNA and protein production that are commonly seen as a cell prepares to divide.

The hypothesis-driven GO analysis grouped the proteins affected by PB into three mechanisms associated with cancer: apoptosis, alteration of cell cycle, and increased metabolism involving cytochromes and/or xenobiotics. The proteins in each group were scored based on whether their functions were pro- or anticancer, quantified based on the direction and magnitude of their fold changes from control and a sum effect calculated for each group (Fig. 2). These GO results suggest that the mechanism of nongenotoxic carcinogenesis involves both increased metabolism, especially induction of the 2B subfamily of CYP enzymes, and increased cell cycle activity. Apoptosis, however, also increased, perhaps, as an attempt to counter the PB cancer threat. Attempts to stimulate apoptosis are also seen in the IPA network analysis described below.

IPA Analysis

The proteins showing significant changes after PB exposure mapped into 13 networks. Networks that had five or more focus genes (gene objects having direct interactions with IPKB database nodes) were considered to be "major" networks. Six major networks were generated (Figs. 3–8) with complete lists of gene objects given in the supplementary tables 3–8. We concentrated on those focus genes most relevant to the aforementioned two theories of nongenotoxic carcinogenesis: increased metabolism which may involve reactive oxygen species as proposed by Dostalek *et al.* (2007) and Elrick *et al.* (2005) or decreased apoptosis with cell cycle dysregulation as suggested by Kolaja *et al.* (2000) and Seidel *et al.* (2006).

Forty-one of the IPA-mapped proteins have functions classified as procarcinogenic according to the hypothesized mechanism of decreases in apoptosis, intercellular communication, tumor suppressor gene function, and DNA repair time plus increased cell proliferation and other aberrant cellular activity (Kolaja *et al.*, 2000; Seidel *et al.*, 2006). Applying the same mechanistic criteria, 14 proteins would be considered anticarcinogenic. This contradicts the earlier hypothesis-driven

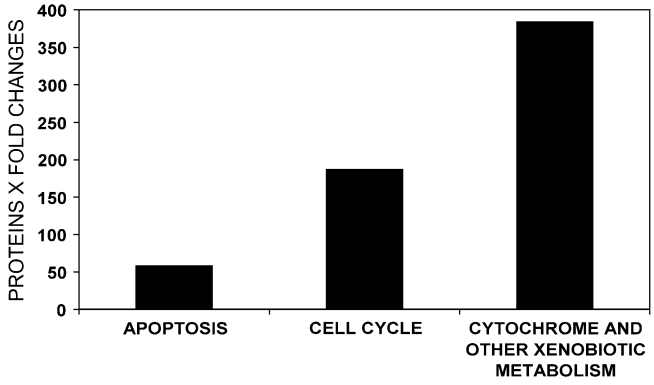

FIG. 2. Comparison of PB protein changes as assigned to three possible nongenotoxic mechanisms of hepatocarcinogenesis suggested by hypothesis-driven GO modeling. Differentially expressed proteins were scored as either agonistic (+ 1), antagonistic (− 1), or no effect (0) for carcinogenesis based on the function of the protein. These scores were then multiplied by the proportional increase or decrease after PB exposure (fold change) to derive a collective quantitative value that represents both the number of proteins associated with each hypothesis and the magnitude of their changes after PB exposure.

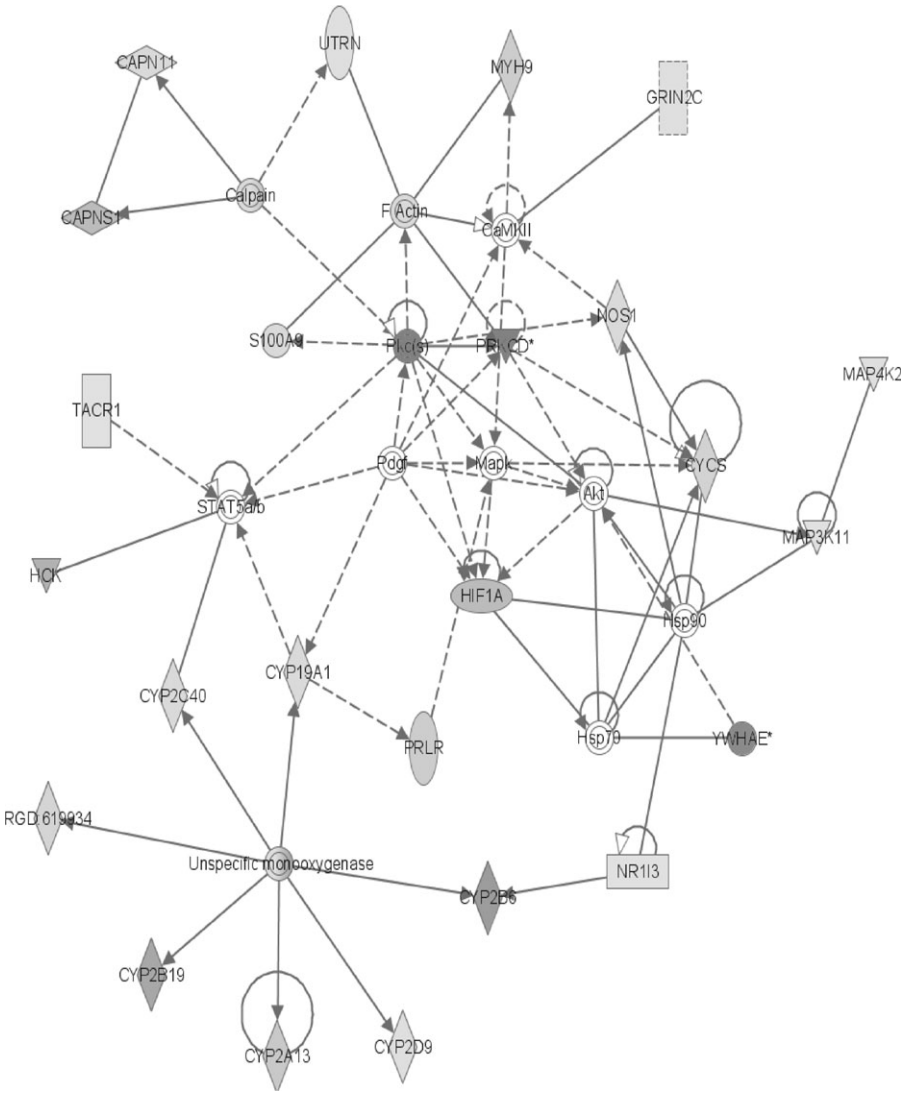

FIG. 3. The network containing the largest number of differentially expressed proteins. The intensity of the shading increases with the magnitude of the change. In the online color version, green represents a decrease and red indicates an increase. Shaded or colored nodes are derived from the 2D LC ESI MS^2 identified protein data set, whereas white nodes are inserted by the IPA program. Complete gene product names are listed in the ''Supplementary Data'' section. Nodes are displayed using various shapes that represent the functional class of the gene product: concentric circles represent a group or complex; down-pointing triangles represent kinases; diamonds stand for other enzymes; horizontal ovals stand for transcription regulators; vertical ovals indicate transmembrane receptors; vertical rectangles represent G-protein–coupled receptors; horizontal rectangles indicate ligand-dependent nuclear receptors; and circles represent other actors. Solid lines indicate direct interactions between nodes and dashed lines indicate indirect interactions. Lines beginning and ending on the same node show self-regulation. Arrowheads show directionality of the relationship. RGD: 619934 is the rat homologue of CYP2C6.

GO results which suggested that there is a total increase in apoptosis. Variation in analysis methods may explain the difference. Since the hypothesis-driven GO analysis factors in the magnitude of the protein changes, its conclusion of a total increase in apoptosis activity is probably a better indicator than simply counting the total number of IPA nodes described in the literature as pro- or antiapoptotic.

Twenty-two additional IPA nodes can be classified as procarcinogenic by the competing theory of increased metabolism resulting in the formation of reactive oxygen species that, in turn, cause cancer (Dostalek *et al*., 2007; Elrick *et al*., 2005).

The first network contains 24 focus genes (Fig. 3). One of the major branches involves an unspecified monooxygenase. From this enzyme, several CYPs radiate and all show the induction characteristic of PB exposure (Waxman and Azaroff, 1992) with six members of CYP family 2 (RGD: 619934 is the rat homologue of CYP2C6) and one member of family 1 showing increased levels. This induction of numerous CYPs, with concomitant increases in metabolism, lends support to the role of oxidative stress in rat nongenotoxic carcinogenicity due to PB exposure (Dostalek *et al*., 2007; Elrick *et al*., 2005). These induced CYPs include the most strongly increased

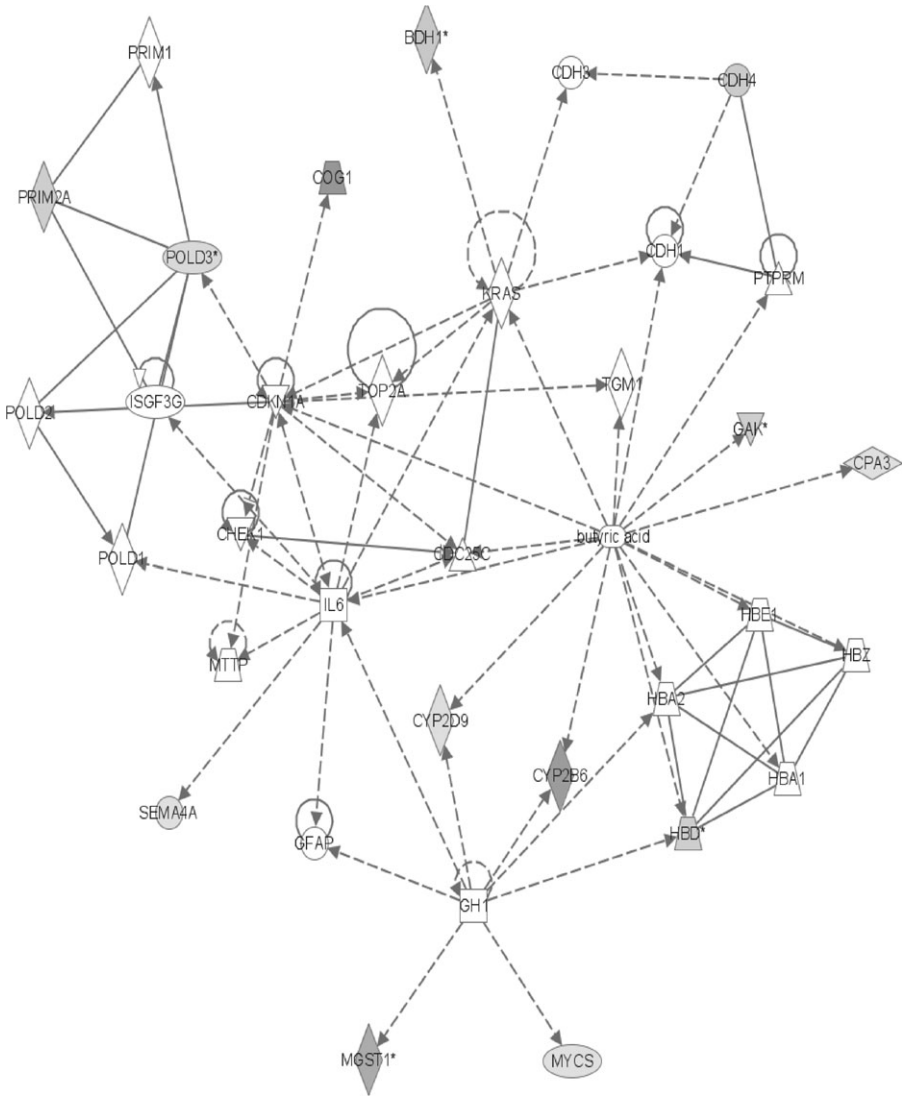

FIG. 4. The network containing the second largest number of differentially expressed proteins. Symbols are as described in the legend for Figure 3 with the addition of squares for cytokines, trapezoids for transporters, and up-pointing triangles for phosphatases.

protein found in the MS data, CYP2B2 (here identified as the human homologue CYP2B6). CYP2B6 metabolizes numerous xenobiotics and its induction by PB is well known (Parkinson, 2001). The present proteomic result of increased CYP2B6 (CYP2B2) agrees with earlier microarray (Seidel *et al*., 2006) and amplified fragment length polymorphism (Elrick *et al*., 2005) data. It is also supported by our earlier work in which CYP2B2 mRNA levels and P450-mediated enzyme activities were increased following the same PB treatment (Dail *et al*., 2007). Additional evidence in the top network for the metabolism/reactive oxygen mechanism of PB hepatocarcinogenesis is suggested by the strong increase in HIF1A which has recently become the focus of intense research regarding antioxidants and cancer. HIF1A causes transcription of proangiogenic factors, and its levels are affected by the concentrations of nitric oxide (NO) and reactive oxygen species present (Wellman *et al*., 2004). HIF1A apparently initiates angiogenesis and helps hypoxic cells convert sugar to energy without oxygen. It is thought that a cancer cell's increased metabolic rate rapidly uses up all the available oxygen and, therefore, requires a functional HIF1A for survival. According to this theory, free radicals do not cause cancer via DNA damage but rather through their support of HIF1A function (Gao *et al*., 2007).

Another of the increased network #1 proteins associated with metabolism is the constitutive active/androstane receptor (CAR/NR1I3). The present IPA shows NR1I3 (CAR) affecting CYP2B6 (Fig. 3). After PB exposure, CAR translocates to the nucleus where it associates with the retinoid X receptor, and they bind to the PB-responsive enhancer module to upregulate the transcription of many CYPs (Timsit and Negishi, 2007),

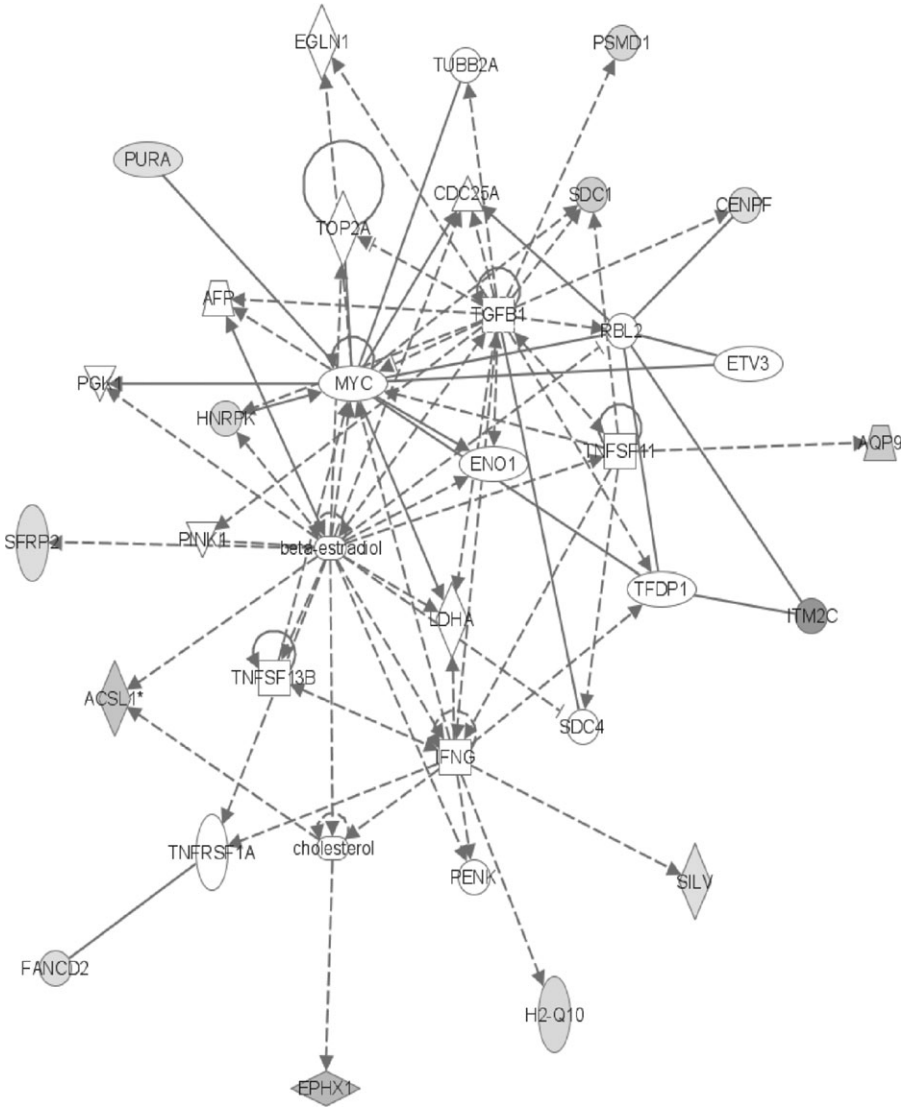

FIG. 5. The network containing the third largest number of differentially expressed proteins. Symbols are as described in the legends for Figures 3 and 4.

thereby increasing metabolic rates and the likely production of reactive oxygen species. Recently, it has been shown that PB treatment also causes translocation of CAR to the cell membrane where it is hypothesized to help in processing the PB signal (Koike *et al*., 2005). If this is accurate, the DDFs generated in this experiment should reflect these CAR translocations. The amount of CAR in different fractions should vary between the saline control and the PB livers. This was, indeed, the case with about three times as much CAR protein being found in the PB nuclear fraction as in the control nuclear fraction. These results also point out that even after nuclear translocation, the majority of CAR protein is still extranuclear and, therefore, available to act at the membrane in a signaling capacity.

Showing a reduced level in the top network is NOS (nitric oxide synthase) which produces nitric oxide (NO) that interacts with a multitude of proteins and reactive oxygen species (Sass *et al*., 2001). This reduction may be viewed as a compensatory effort to balance the increased metabolic production of reactive oxygen species. An additional compensatory response is seen in the second network (Fig. 4) with the increase of microsomal glutathione *S*-transferase (MGST1) which is thought to protect against oxidative and nitrosative stress as its level of enzymatic activity increases in the presence of oxidants and NO donors (Yanbin *et al*., 2002). The increase in epoxide hydrolase (EPHX1) seen in network #3 (Fig. 5) may also be a response to the increased activity of the CYP oxidative enzymes seen earlier in networks #1 and #2 (Figs. 3 and 4). An increase in EPHX1 decreases the chance for DNA and protein damage from the liver's endogenous epoxide production and, therefore, decreases the PB-related cancer risk. This is thought to be part

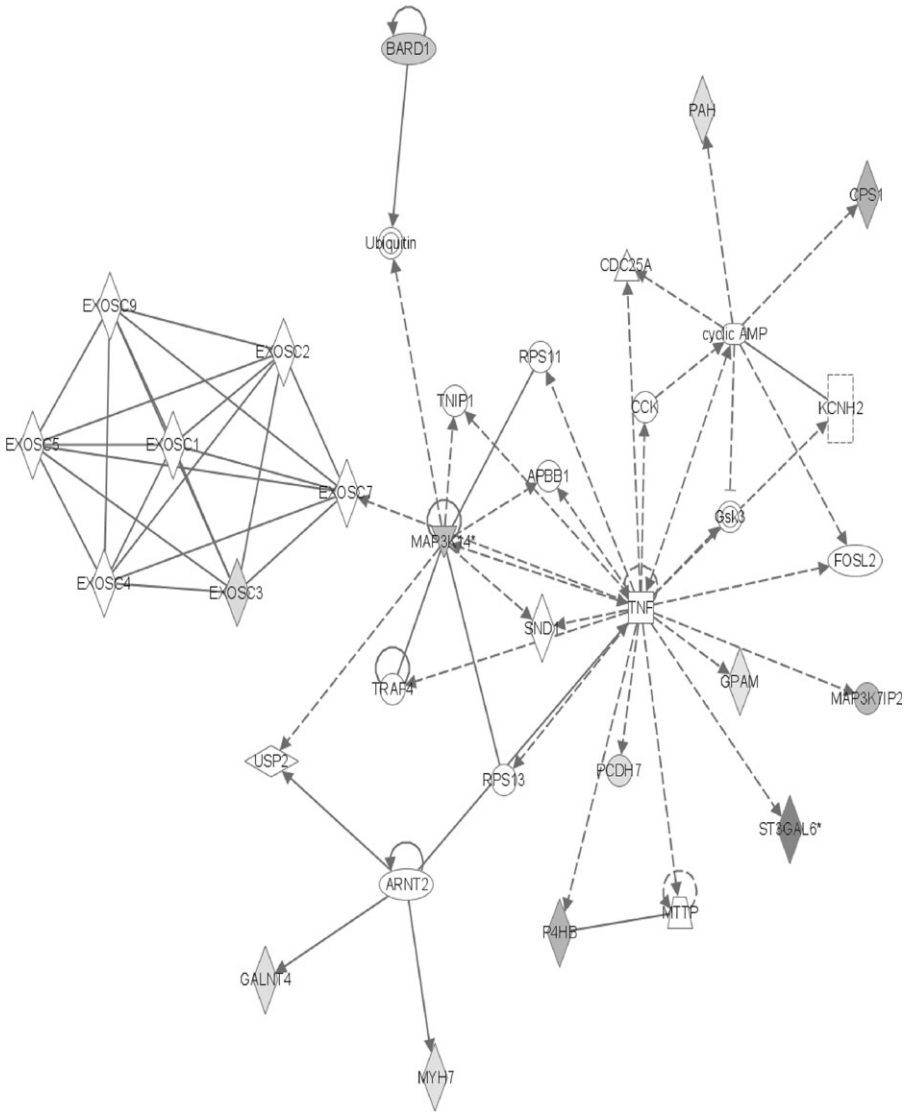

FIG. 6. The network containing the fourth largest number of differentially expressed proteins. Symbols are as described in the legends for Figures 3 and 4.

of the reason Sonzogni *et al*. (2002) frequently found reduced EPHX1 enzymatic activity in patients with hepatocellular carcinoma.

The last section of network #5 is a group of glucuronosyltransferases, all of which show significant increases over control values (Fig. 7). According to the Integrated Enzyme Database (http://www.ebi.ac.uk/intenz/), this group encompasses 51 separate enzymes acting upon a wide variety of substrates, and their delineation is still being determined. This confusion may explain the fact that UGTB37 is shown with an asterisk that, according to the IPA program, indicates that duplicate gene list data set entries were merged into a single gene found in the IPKB literature. The glucuronosyltransferase nomenclature confusion plus the IPKB bundling may explain some observed inconsistencies. The data show the UDP-glucuronosyltransferase 2B2 precursor as increasing almost 77-fold and also as decreasing almost 20-fold following PB exposure. This protein was the only toxicologically relevant protein to have shown statistically significant decreased expression. It appears that this confusion may be the result of an error in identifying the correct form of glucuronosyltransferase. Also even though the MS data indicated increases in the rat proteins UGT2B2 and UGT2B5, the IPA network shows mouse proteins UGT2B5 and UGT2B37. Mouse UGT2B5 shares homology with the rat protein UGT2B3, not UGT2B2 or UGT2B5 (Eppig *et al*., 2005). Mouse UGT2B37 has no rat orthologues (Eppig *et al*., 2005; Twigger *et al*., 2007), yet the IPA considers it to be synonymous with rat UGT2B2. Despite these nomenclature problems, the data indicate that PB does increase the amount of the important phase 2 glucuronosyltransferases, which is consistent with prior work (Parkinson and Ogilvie, 2008).

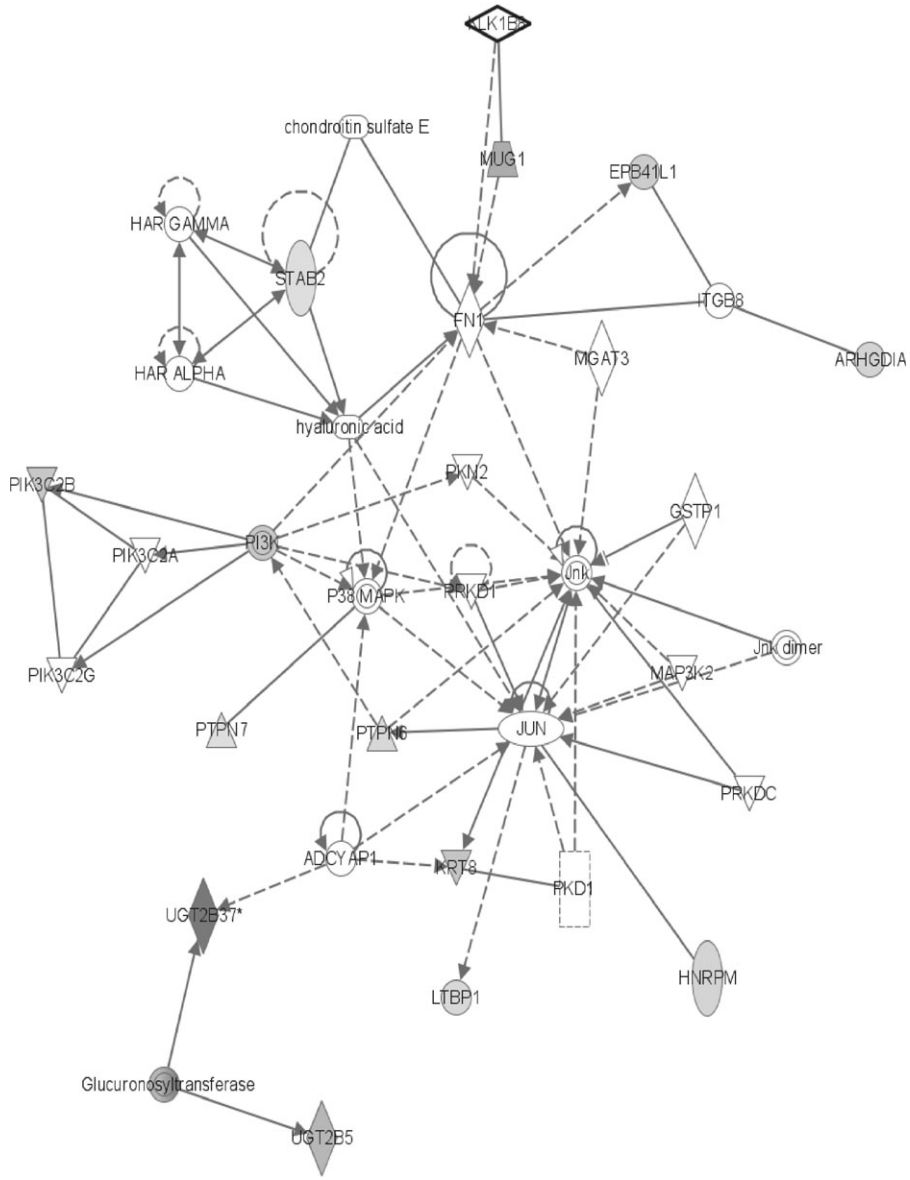

FIG. 7. The network containing the fifth largest number of differentially expressed proteins. Symbols are as described in the legends for Figures 3 and 4.

Many more IPA nodes seemed to be associated with changes in apoptosis and the cell cycle than increases in metabolism. In some cases, overlap occurs as is the case with CYP2B19 and CYP2C40 which are both involved in xenobiotic metabolism and the production of epoxyeicosatrienoic acids (EETs) (Du *et al*., 2005; Tsao *et al*., 2000). EET is involved in aberrant cellular differentiation, signal transduction pathways, the regulation of cell proliferation, survival, migration, growth, and mitogenesis (Ladd *et al*., 2003). The observed increases in CYP2B19 and CYP2C40 could, therefore, be seen as supporting both the increased metabolism and the cell dysregulation theories of carcinogenesis.

Several other network #1 nodes have links to apoptosis and/or the cell cycle (Fig. 3). Two members of the mitogen-activated protein kinase family, which regulates numerous processes including proliferation, differentiation, and apoptosis (Qi and Elion, 2005), are also shown as induced in the top network (Fig. 3). MAP3K11 has been shown to induce proliferation and transformation in nonneuronal cells (Nguyen *et al*., 2007). MAP4K2 regulates eukaryotic stress responses (Kyriakis, 1999). The fact that calpain (CAPN) is shown as being both induced and repressed is possibly related to the induction of CAPNS1 and the repression of CAPN11 with which it interacts (Fig. 3). Induction of CAPNS1 has been linked to increased nuclear factor kappa B (NF-κB) activation with a resultant decrease in apoptosis (Demarchi *et al*., 2005). A decrease in apoptosis may also be the result of the observed decrease in CAPN11 (Ben-Aharon *et al*., 2006). PRKCD, the delta isoform

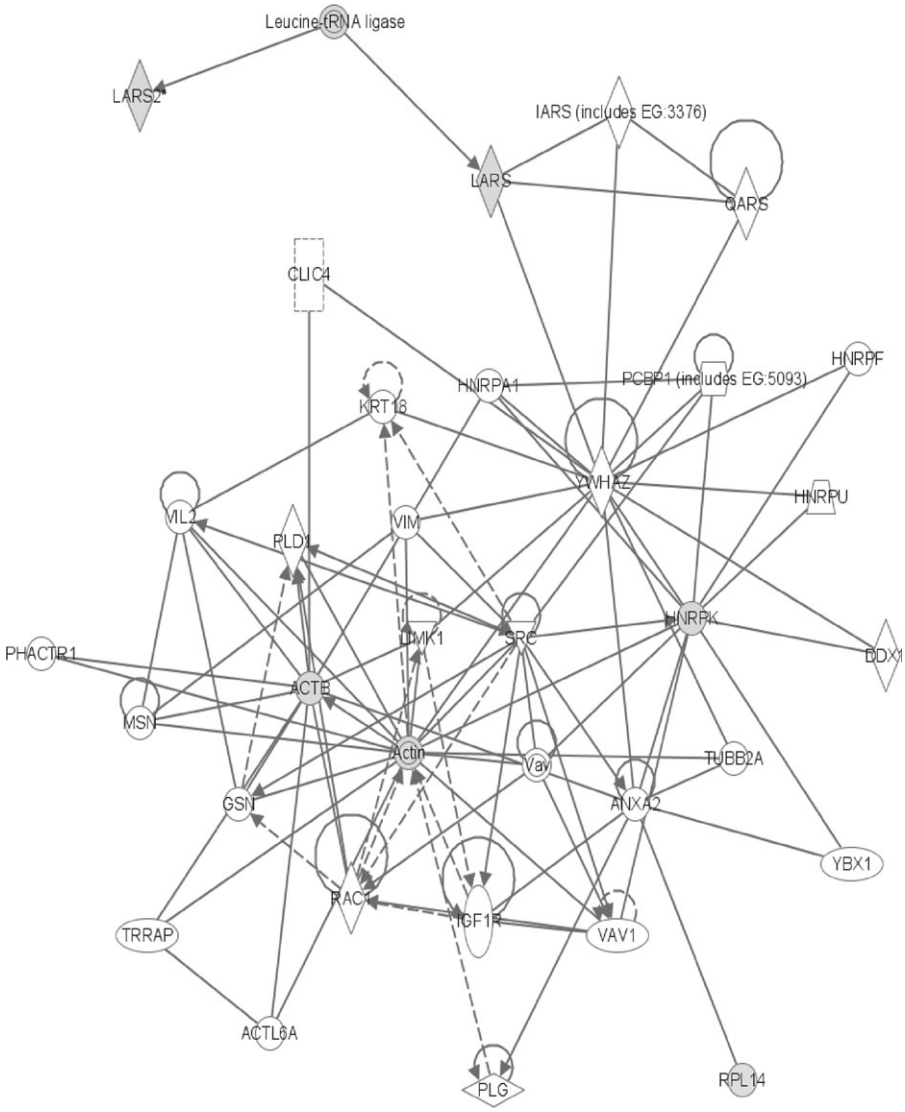

FIG. 8. The network containing the sixth largest number of differentially expressed proteins. Symbols are as described in the legends for figures 3 and 4.

of protein kinase C, normally stimulates apoptotic cell death after it is activated (Yoshida, 2007), so its decrease here may also suggest a further reduction in apoptosis. As PRKCD is also implicated in causing mitochondrial release of cytochrome c (CYCS) (Yoshida, 2007), the same decrease may relate to the observed decrease of CYCS seen in network #1 (Fig. 3). Because cytochrome c's translocation from the mitochondria to the cytosolic apoptosome complex helps trigger the apoptotic cascade (Bertini *et al*., 2006), its reduction could inhibit apoptosis. As described above for CAR, the DDF method allows for cytochrome c's localization. In the control group, CYCS is evenly divided between the mitochondrial and cytosolic fractions, whereas after PB exposure CYCS is only found in the cytosolic fraction, suggesting an initiation of apoptosis in response to the treatment. This agrees with our previous hypothesis-driven GO-based analysis. Other network #1 nodes also show attempts to compensate for the effects of PB. The amount of prolactin receptor (PRLR) decreased. PRLR has been associated with the inhibition of apoptosis in breast cancer cells (Kline *et al*., 1999), so its decrease here could stimulate apoptosis. However, many different isoforms of PRLR exist with varying functions in different tissues. Kline *et al*. (1999) found that the rat intermediate and long PRLR homodimers were associated with the inhibition of apoptosis, whereas the heterodimeric isoforms were not. Perhaps, the homodimeric forms are decreasing here. YWHAE, also known as 14-3-3, is a cruciform DNA-binding protein which showed reduced levels after PB exposure. It is involved in initiation of DNA replication, regulation of transcription, cell cycle progression, and signal transduction (Yahyaoui *et al*., 2007), so its

reduction here may be a sign of a compensatory effort to slow down the cell cycle.

The second network shows several responses that can be construed as antiapoptotic or altering the cell cycle (Fig. 4). The level of S-myc protein from the myc-like oncogene (MYCS) was decreased by PB exposure, and since S-myc induces apoptosis and suppresses tumors (Noguchi *et al*., 2000), these processes become less likely. BDH1 is D-beta-hydroxybutyrate dehydrogenase and its observed increase would likely cause an increased metabolism of butyrate and its analogues such as butyric acid seen in another node of this network (Takanashi and Saito, 2006). A reduction in available butyrate causes a decrease in apoptosis and an increase in the rate of tumor growth (Huang *et al*., 1999). Both PRIMA and POLD3 are involved in the mechanics of DNA replication (Shiratori *et al*., 1995; Shultz *et al*., 2007). Since the amounts of both are increased after PB treatment, it is reasonable to suspect that an increase in the amount of DNA replication may be occurring that is conducive to an increased rate of cell cycle progression.

Network #3 has a number of nodes that involve cell cycle progression and/or cell division (Fig. 5). Centromere protein-F (CENPF) is a kinetochore protein that associates with the chromosomal centromere and connects the mitotic spindle microtubules, thereby allowing the chromosomes to align at metaphase and separate at anaphase (Liao *et al*., 1995). Since CENPF normally degrades quickly after cells complete mitosis, its increased level here may hint at an increasing rate of mitosis. Purine-rich element binding protein A (PURA) is involved in DNA replication and transcription plus regulation of cell cycle progression (Darbinian *et al*., 2001). Since an increase in PURA inhibited cell growth (Darbinian *et al*., 2001), it is likely that its observed decrease could promote cellular proliferation in the PB-exposed rat. Likewise, the heterogeneous nuclear ribonucleoprotein K (HNRPK) can inhibit translation from starting (Ostareck-Lederer and Ostareck, 2004), so its decrease here may result in increased rates of translation. On the other hand, the increased amount of FANCD2, a downstream protein of the Fanconi anemia pathway, may be prohibiting tumor formation since it has been shown to promote homology-directed repair of chromosomal double-strand DNA breaks (Nakanishi *et al*., 2005). The Fanconi anemia gene is considered to be a DNA damage response gene, and mutations in it have been linked to leukemia and lymphoma (Curtin *et al*., 2007).

The fourth major network contains several nodes exhibiting changes that may be considered as anticancer (Fig. 6). Enhanced production of BRCA1-associated RING domain 1 (BARD1) protein has been found in breast and ovarian tumors (Li *et al*., 2007), where it is thought to both stabilize the tumor suppressor BRCA1 and, independently, stimulate apoptosis. Its increase here would seem to suppress tumor formation. The reduction of MAP3K14 can also be construed as an attempt to prevent cancer since it induces NF-κB activity (Mallnin *et al*., 1997). Because NF-κB can increase proliferation and inflammation while inhibiting apoptosis (Gregus and Klaassen, 2001), a decrease in any of its inducers should lower the cancer risk. The same can be said for the observed decrease in MAP3K7IP2, also known as TAB2. MAP3K7IP2 complexes with tumor necrosis factor receptor–associated factor 6 and transforming growth factor-beta–activating kinase-1 to stimulate NF-κB and the c-Jun NH_2-terminal kinase (Schlessinger and Lemmon, 2006; Yokota *et al*., 2008) which can both increase proliferation, inflammation, and apoptosis.

Network #5 again shows pro- and anticancer responses (Fig. 7). Protein tyrosine phosphatase, non-receptor type 6 (PTPN6) is also known as Src homology 2 domain–containing tyrosine phosphatase 1 (SHP-1). Lack of SHP-1 has been linked to increased cell production, and reduced expression of SHP-1 is common to many lymphomas and leukemias (Wang *et al*., 2006), so its decrease here may indicate a trend toward cancer. Phosphoinositide-3-kinase (PI3K) represents a family of lipid kinases which produce lipids capable of regulating proteins involved in cell proliferation and apoptosis (Falasca *et al*., 2007). One member of this family is phosphoinositide-3-kinase, class 2, beta polypeptide (PIK3C2β) whose activity increases during compensatory liver growth (Sinđić *et al*., 2001), so the increase seen here is logical. ARHGDIA is a synonym for RHO GDIα which is an inhibitor that binds to all the RHO proteins, and since active RHO GTPase is needed for cell proliferation (Wei *et al*., 2002), the observed increase of its inhibitor, RHO GDIα, should slow carcinogenesis. Decreasing keratin 8 (KRT8) levels, as seen here, have been correlated with increased apoptosis (Galarneau *et al*., 2007).

Finally, the gene for the human version of RPL14 (60S ribosomal subunit protein L14) (Fig. 8) was first isolated by screening for genes responsible for cellular immortality, proliferation, and strong protein synthesis (Tanaka *et al*., 1998). Its increase in network #6 lends additional support to the cell cycle theory of nongenotoxic carcinogenesis.

In conclusion, it appears that global mass spectrophotometric proteomic analysis may be useful at identifying chemicals with carcinogenic potential at a very early stage. The level of PB exposure in this study was below that required to damage the liver as indicated by a diagnostic serum hepatic enzyme panel (Dail *et al*., 2007), and yet a large number of CYP enzymes and other proteins related to increased oxidative stress were identified as altered after just 5 days of exposure using a small number of animals. The present CYP results were in excellent agreement with earlier work using both classic microsomal enzyme assays and the newer quantitative reverse transcription-PCR methods (Dail *et al*., 2007) with the main difference being the large amount of additional information generated by the global proteomic analysis. The protein changes involving apoptosis are not as clear cut since some indicate increased apoptosis and others suggest that it is decreased. This may suggest that the oxidative stress theory is a more valid mechanism for the nongenotoxic effects of PB or it may indicate a homeostatic attempt to induce apoptosis that is ultimately insufficient to overcome the numerous procarcinogenic changes. In spite of

the mixed apoptosis results, this method seems to be a good candidate for future use in the analysis of chemicals that cause procarcinogenic changes in proteins associated with DNA repair and cell cycle dysregulation since GO and IPA indicated similar changes in these areas. The fact that the IPA analysis indicated 63 proteins that changed in a procarcinogenic manner versus 14 which experienced anticarcinogenic changes suggests that this method correctly indicated the carcinogenic potential of PB and that this method could be useful in the analysis of novel and less well-studied xenobiotics especially when the reduction in time and costs over the traditional 2-year rat carcinogenicity test are factored in. This method could also be used in the initial identification of pathways involved with follow-up work to precisely determine the changes in functional balance that result from the observed changes in protein expression. It may also be useful in investigating the cross-species extrapolation question of why PB does not cause nongenotoxic hepatocarcinogenesis in humans by comparing the protein changes seen in treated human liver cell lines to those seen in the present study. Widespread use of global proteomic techniques in toxicology could lead to the development of "proteome signatures" characteristic of various toxicological end points. Because of these possibilities, we suggest that this approach might be a more efficient way of quickly identifying candidate drugs during discovery that might ultimately prove to be carcinogenic or display other chronic toxicities, so that they might be removed from consideration earlier than is now possible with traditional *in vivo* long-term tests.

FUNDING

National Institutes of Health: Centers of Biomedical Research Excellence (P20-RR017661); Mississippi State University Center for Environmental Health Sciences; Mississippi Agricultural and Forestry Experiment Station.

SUPPLEMENTARY DATA

Supplementary tables 1–8 are available online at http://toxsci.oxfordjournals.org/.

ACKNOWLEDGMENTS

The authors wish to thank Dr. Fiona McCarthy, Dr. Bindu Nanduri, and Ms. Amanda Cooksey for their advice and assistance with the GO and IPA analyses and their suggestions during the preparation of this article. The authors wish to acknowledge the technical expertise and instruction received from the Life Sciences and Biotechnology Institute. The authors also wish to thank Mr. Edward Meek and Mr. Shane Bennett for their fine technical assistance. This article is Center for Environmental Health Sciences publication #120 and Mississippi Agricultural and Forestry Experiment Station publication #J-11385.

REFERENCES

Allen, E. B., Burgess, S. C., and Nanduri, B. (2006). Software applications for integration and analysis of mass spectroscopy data. In *54th ASMS Conference on Mass Spectrometry,* 28 May–1 June, 2006, Seattle, WA.

Amacher, D. E., Adler, R., Herath, A., and Townsend, R. R. (2005). Use of proteomic methods to identify serum biomarkers associated with rat liver toxicity or hypertrophy. *Clin. Chem.* **51,** 1796–1803.

Ashburner, M., Ball, C. A., Blake, J. A., Botstein, D., Butler, H., Cherry, J. M., Davis, A. P., Dolinski, K., Dwight, S. S., Eppig, J. T., *et al.* (2000). Gene Ontology: Tool for the unification of biology. *Nat. Genet.* **25,** 25–29.

Ben-Aharon, I., Brown, P. R., Shalgi, R., and Eddy, E. M. (2006). Calpain 11 is unique to mouse spermatogenic cells. *Mol. Reprod. Dev.* **73,** 767–773.

Bertini, I., Grassi, E., Luchinat, C., Quattrone, A., and Saccenti, E. (2006). Monomorphism of human cytochrome C. *Genomics* **88,** 669–672.

Biswas, S. J., Pathak, S., and Khuda-Bukhsh, A. R. (2004). Assessment of the genotoxic and cytotoxic potential of an anti-epileptic drug, phenobarbital, in mice: A time course study. *Mutat. Res.* **563,** 1–11.

Bridges, S. M., Magee, G. B., Wang, N., Williams, W. P., Burgess, S. C., and Nanduri, B. (2007). ProtQuant: A tool for the label-free quantification of MudPIT proteomics data. *BMC Bioinformatics* **8,** S24.

Buza, J. J., and Burgess, S. C. (2007). Modeling the proteome of a Marek's disease transformed cell line: A natural animal model for CD30 over-expressing lymphomas. *Proteomics* **7,** 1316–1326.

Chen, M., Ying, W., Song, Y., Liu, X., Yang, B., Wu, S., Jiang, Y., Cai, Y., He, F., and Qian, X. (2007). Analysis of human liver proteome using replicate shotgun strategy. *Proteomics* **7,** 2479–2488.

Corcos, L., and Lagadic-Gossman, D. (2001). Gene induction by phenobarbital: An update on an old question that receives key novel answers. *Pharmacol. Toxicol.* **89,** 113–122.

Curtin, C., Dublin, M., Salisbury, M., and Swanson, J. (2007). Cracking the cancer code. In *Genome Technology,* Available at: http://www.genome-technology.com/issues/2_3/webreprints/143738-1.html. Accessed April 1, 2007.

Dail, M. B., Burgess, S. C., Meek, E. C., Wagner, J., Baravik, J., and Chambers, J. E. (2007). Spatial distribution of CYP2B1/2 messenger RNA within the rat liver acinus following exposure to the inducers phenobarbital and dieldrin. *Toxicol. Sci.* **99,** 35–42.

Darbinian, N., Gallia, G. L., King, J., Del Valle, L., Johnson, E. M., and Khalili, K. (2001). Growth inhibition of glioblastoma cells by human Purα. *J. Cell. Physiol.* **189,** 334–340.

Demarchi, F., Bertoli, C., Greer, P. A., and Schneider, C. (2005). Ceramide triggers an NF-κB-dependent survival pathway through calpain. *Cell Death Differ.* **12,** 512–522.

Desiere, F., Deutsch, E. W., Nesvizhskii, A. I., Mallick, P., King, N. L., Eng, J. K., Adarem, A., Boyle, R., Brunner, E., Donohoe, S., *et al.* (2004). Integration with the human genome of peptide sequences obtained by high-throughput mass spectrometry. *Genome Biol.* **6,** R9.

Dostalek, M., Brooks, J. D., Hardy, K. D., Milne, G. L., Moore, M. M., Sharma, S., Morrow, J. D., and Guengerich, F. P. (2007). *In vivo* oxidative damage in rats is associated with barbiturate response but not other cytochrome P450 inducers. *Mol. Pharmacol.* **72,** 1419–1424.

Du, L., Yermalitsky, V., Ladd, P. A., Capdevila, J. H., Mernaugh, R., and Keeney, D. S. (2005). Evidence that cytochrome P450 CYP2B19 is the major source of epoxyeicosatrienoic acids in mouse skin. *Arch. Biochem. Biophys.* **435,** 125–133.

Elias, J. E., and Gygi, S. P. (2007). Target-decoy search strategy for increased confidence in large-scale protein identifications by mass spectrometry. *Nat. Methods* **4,** 207–214.

Elrick, M. M., Kramer, J. A., Alden, C. L., Blomme, E. A. G., Bunch, R. T., Cabonce, M. A., Curtiss, S. W., Kier, L. D., Kolaja, K. L., Rodi, C. P., *et al.* (2005). Differential display in rat livers treated for 13 weeks with phenobarbital implicates a role for metabolic and oxidative stress in nongenotoxic carcinogenicity. *Toxicol. Pathol.* **33,** 118–126.

Eppig, J. T., Bult, C. J., Kadin, J. A., Richardson, J. E., and Blake, J. A. (2005). The members of the Mouse Genome Database Group. (2005). The Mouse Genome Database (MGD): From genes to mice—A community resource for mouse biology. *Nucleic Acids Res.* **33,** D471–D475.

Falasca, M., Hughes, W. E., Dominguez, V., Sala, G., Fostira, F., Fang, M. Q., Cazzoli, R., Shepherd, P. R., James, D. E., and Maffucci, T. (2007). The role of phosphoinositide 3-kinase C2alpha in insulin signaling. *J. Biol. Chem.* **282,** 28226–28236.

Galarneau, L., Loranger, A., Gilbert, S., and Marceau, N. (2007). Keratins modulate hepatic cell adhesion, size and G1/S transition. *Exp. Cell Res.* **313,** 179–194.

Galeva, N., Yakovlev, D., Koen, Y., Duzhak, T., and Alterman, M. (2003). Direct identification of cytochrome P450 isozymes by matrix-assisted laser desorption/ionization time of flight-based proteomic approach. *Drug Metab. Dispos.* **31,** 351–355.

Gao, P., Zhang, H., Dinavahi, R., Li, F., Xiang, Y., Raman, V., Bhujwalla, Z. M., Felsher, D. W., Cheng, L., Pevsner, J., *et al.* (2007). HIF-dependent antitumorigenic effect of antioxidants *in vivo*. *Cancer Cell* **12,** 230–238.

Gerhold, D., Lu, M., Xu, J., Austin, C., Caskey, C. T., and Rushmore, T. (2001). Monitoring expression of genes involved in drug metabolism and toxicology using DNA microarrays. *Physiol. Genomics* **5,** 161–170.

Gregus, Z., and Klaassen, C. D. (2001). Mechanisms of toxicity. In *Casarett and Doull's Toxicology: The Basic Science of Poisons* (C. D. Klaassen, Ed.), pp. 35–81. McGraw-Hill, New York, NY.

Guenther, M. G., Levine, S. S., Boyer, L. A., Jaenisch, R., and Young, R. A. (2007). A chromatin landmark and transcription initiation at most promoters in human cells. *Cell* **130,** 77–88.

Gygi, S. P., Rochon, Y., Franza, B. R., and Aebersold, R. (1999). Correlation between protein and mRNA abundance in yeast. *Mol. Cell. Biol.* **19,** 1720–1730.

Hamadeh, H. K., Bushel, P. R., Jayadev, S., DiSorbo, O., Bennett, L., Li, L., Tennant, R., Stoll, R., Barrett, J. C., Paules, R. S., *et al.* (2002). Prediction of compound signature using high density gene expression profiling. *Toxicol. Sci.* **67,** 232–240.

Huang, H., Reed, C. P., Zhang, J., Shridhar, V., Wang, L., and Smith, D. I. (1999). Carboxypeptidase A3 (CPA3): A novel gene highly induced by histone deacetylase inhibitors during differentiation of prostate epithelial cancer cells. *Cancer Res.* **59,** 2981–2988.

Jiang, X., Zhou, H., Zhang, L., Sheng, Q., Li, S., Li, L., Hao, P., Li, Y., Xia, Q., Wu, J., *et al.* (2004). A high-throughput approach for subcellular proteome: Identification of rat liver proteins using subcellular fractionation coupled with two-dimensional liquid chromatography tandem mass spectrometry and bioinformatics analysis. *Mol. Cell. Proteomics* **3,** 441–455.

Kakizaki, S., Yamamoto, Y., Ueda, A., Moore, R., Sueyoshi, T., and Negishi, M. (2003). Phenobarbital induction of drug/steroid-metabolizing enzymes and nuclear receptor CAR. *Biochim. Biophys. Acta* **1619,** 239–242.

Kier, L. D., Neft, R., Tang, L., Suizu, R., Cook, T., Onsurez, K., Tiegler, K., Sakai, Y., Ortiz, M., Nolan, T., *et al.* (2004). Applications of microarrays with toxicologically relevant genes (tox genes) for the evaluation of chemical toxicants in Sprague Dawley rats *in vivo* and human hepatocytes in vitro. *Mutat. Res. Fundam. Mol. Mech. Mutagen.* **549,** 101–113.

Kiyosawa, N., Tanaka, K., Hirao, J., Ito, K., Niino, N., Sakuma, K., Kanbori, M., Yamoto, T., Manabe, S., and Matsunuma, N. (2004). Molecular mechanism investigation of phenobarbital-induced serum cholesterol elevation in rat livers by microarray analysis. *Arch. Toxicol.* **78,** 435–442.

Kline, J. B., Roehrs, H., and Clevenger, C. V. (1999). Functional characterization of the intermediate isoforms of the human prolactin receptor. *J. Biol. Chem.* **274,** 35461–35468.

Koike, C., Moore, R., and Negishi, M. (2005). Localization of the nuclear receptor CAR at the cell membrane of mouse liver. *FEBS Lett.* **579,** 6733–6736.

Kolaja, K. L., Engelken, D. T., and Klaassen, C. D. (2000). Inhibition of gap-junctional-intercellular communication in intact rat liver by nongenotoxic hepatocarcinogens. *Toxicology* **146,** 15–22.

Kyriakis, J. M. (1999). Signaling by the germinal center kinase family of protein kinases. *J. Biol. Chem.* **274,** 5259–5262.

Ladd, P. A., Du, L., Capdevila, J. H., Mernaugh, R., and Keeney, D. S. (2003). Epoxyeicosatrienoic acids activate transglutaminases *in situ* and induce cornification of epidermal keratinocytes. *J. Biol. Chem.* **278,** 35184–35192.

Leone, A. M., Kao, L. M., McMillian, M. K., Nie, A. Y., Parker, J. B., Kelley, M. F., Usuki, E., Parkinson, A., Lord, P. G., and Johnson, M. D. (2007). Evaluation of felbamate and other antiepileptic drug toxicity potential based on hepatic protein covalent binding and gene expression. *Chem. Res. Toxicol.* **20,** 600–608.

Li, D., He, Y., Guo, Y., Wang, F., Song, S., Wang, Y., Yang, F., He, X., and Sun, S. (2007). Comparative proteomics analysis to annexin B1 DNA and protein vaccination in mice. *Vaccine* **25,** 932–938.

Liao, H., Winkfein, R. J., Mack, G., Rattner, J. B., and Yen, T. J. (1995). CENP-F is a protein of the nuclear matrix that assembles onto kinetochores at late G2 and is rapidly degraded after mitosis. *J. Cell Biol.* **130,** 507–518.

Link, A. J., Eng, J., Schieltz, D. M., Carmack, E., Mize, G. J., Morris, D. R., Garvik, B. M., and Yates, J. R., III. (1999). Direct analysis of protein complexes using mass spectrometry. *Nat. Biotechnol.* **17,** 676–682.

Ma, T., and Chambers, J. E. (1995). A kinetic analysis of hepatic microsomal activation of parathion and chlorpyrifos in control and phenobarbital-treated rats. *J. Biochem. Toxicol.* **10,** 63–68.

MacCoss, M. J., Wu, C. C., and Yates, J. R. (2002). Probability-based validation of protein identifications using a modified SEQUEST algorithm. *Anal. Chem.* **74,** 5593–5599.

Mallnin, N. L., Boldin, M. P., Kovalenko, A. V., and Wallach, D. (1997). MAP3K-related kinase involved in NF-κB induction by TNF, CD95 and IL-1. *Nature* **385,** 540–544.

McCarthy, F. M., Bridges, S. M., and Burgess, S. C. (2007). GOing from functional genomics to biological significance. *Cytogenet. Genome Res.* **117,** 278–287.

McCarthy, F. M., Burgess, S. C., van den Berg, B. H., Koter, M. D., and Pharr, G. T. (2005). Differential detergent fractionation for non-electrophoretic eukaryote cell proteomics. *J. Proteome Res.* **4,** 316–324.

McCarthy, F. M., Cooksey, A. M., Wang, N., Bridges, S. M., Pharr, G. T., and Burgess, S. C. (2006b). Modeling a whole organ using proteomics: The avian bursa of Fabricius. *Proteomics* **6,** 2759–2771.

McCarthy, F. M., Wang, N., Magee, G. B., Nanduri, B., Lawrence, M. L., Camon, E. B., Burrell, D. G., Hill, D. P., Dolan, M. E., Williams, W. P., *et al.* (2006a). AgBase: A functional genomics resource for agriculture. *BMC Genomics* **7,** 229–242.

Nakanishi, K., Yang, Y., Pierce, A. J., Taniguchi, T., Digweed, M., Ď Andrea, A. D., Wang, Z., and Jasin, M. (2005). Human Fanconi anemia monoubiquitination pathway promotes homologous DNA repair. *Proc. Natl. Acad. Sci. U.S.A.* **102,** 1110–1115.

Nanduri, B., Lawrence, M. L., Vanguri, S., and Burgess, S. C. (2005). Proteomic analysis using an unfinished bacterial genome: The effects of subminimum inhibitory concentrations of antibiotics on Mannheimia haemolytica virulence factor expression. *Proteomics* **5,** 4852–4863.

Nesvizhskii, A. I., Keller, A., Kolker, E., and Abersold, R. (2003). A statistical model for identifying proteins by tandem mass spectrometry. *Anal. Chem.* **75,** 4646–4658.

Nguyen, D. G., Yin, H., Zhou, Y., Wolff, K. C., Kuhen, K. L., and Caldwell, J. S. (2007). Identification of novel therapeutic targets for HIV infection through functional genomic cDNA screening. *Virology* **362,** 16–25.

Nie, A. Y., McMillian, M., Parker, J. B., Leone, A., Bryant, S., Yieh, L., Bittner, A., Nelson, J., Carmen, A., Wan, J., and Lord, P. G. (2006). Predictive toxicogenomics approaches reveal underlying molecular mechanisms of nongenotoxic carcinogenicity. *Mol. Carcinog.* **45,** 914–933.

Nisar, S., Lane, C. S., Wilderspin, A. F., Welham, K. J., Griffiths, W. J., and Patterson, L. H. (2004). A proteomic approach to the identification of cytochrome P450 isoforms in male and female rat liver by nanoscale liquid chromatography-electrospray ionization-tandem mass spectrometry. *Drug Metab. Dispos.* **32,** 382–386.

Noguchi, K., Yamana, H., Kitanaka, C., Mochizuki, T., Kokubu, A., and Kuchino, Y. (2000). Differential role of the JNK and p38 MAPK pathway in c-Myc- and s-Myc-mediated apoptosis. *Biochem. Biophys. Res. Commun.* **267,** 221–227.

Oliver, J. D., and Roberts, R. A. (2002). Receptor-mediated hepatocarcinogenesis: Role of hepatocytes proliferation and apoptosis. *Pharmacol. Toxicol.* **91,** 1–7.

Ostareck-Lederer, A., and Ostareck, D. H. (2004). Control of mRNA translation and stability in haematopoietic cells: The function of hnRNPs K and E1/E2. *Biol. Cell* **96,** 407–411.

Parkinson, A. (2001). Biotransformation of xenobiotics. In *Casarett and Doull's Toxicology: The Basic Science of Poisons*, 6th ed. (C. D. Klaassen, Ed.), pp. 133–224. McGraw-Hill, New York, NY.

Parkinson, A., and Ogilvie, B. W. (2008). Biotransformation of xenobiotics. In *Casarett and Doull's Toxicology: The Basic Science of Poisons*, 7th ed. (C. D. Klaassen, Ed.), pp. 161–304. McGraw-Hill, New York, NY.

Qi, M., and Elion, E. A. (2005). MAP kinase pathways. *J. Cell Sci.* **118,** 3569–3572.

Ramsby, M. L., Makowski, G. S., and Khairallah, E. A. (1994). Differential detergent fractionation of isolated hepatocytes: Biochemical, immunochemical and two-dimensional gel electrophoresis characterization of cytoskeletal and noncytoskeletal compartments. *Electrophoresis* **15,** 265–277.

Sass, G., Koerber, K., Bang, R., Guehring, H., and Tiegs, G. (2001). Give me iNOS or give me death. *Hepatology* **34,** 436–437.

Schlessinger, J., and Lemmon, M. A. (2006). Nuclear signaling by receptor tyrosine kinases: The first robin of spring. *Cell* **127,** 45–48.

Seidel, S. D., Stott, W. T., Kan, H. L., Sparrow, B. R., and Gollapudi, B. B. (2006). Gene expression dose-response of liver with a genotoxic and nongenotoxic carcinogen. *Int. J. Toxicol.* **25,** 57–64.

Shiratori, A., Okumura, K., Nogami, M., Taguchi, H., Onozaki, T., Inoue, T., Ando, T., Shibata, T., Izumi, M., Miyazawa, H., *et al.* (1995). Assignment of the 49-kDa (PRIM1) and 58-kDa (PRIM2A and PRIM2B) subunit genes of the human DNA primase to chromosome bands 1q44 and 6p11.1-p12. *Genomics* **28,** 350–353.

Shultz, R. W., Tatineni, V. M., Hanley-Bowdoin, L., and Thompson, W. F. (2007). Genome-wide analysis of the core DNA replication machinery in the higher plants Arabidopsis and rice. *Plant Physiol.* **144,** 1697–1714.

Sinđić, A., Aleksandrova, A., Fields, A. P., Volinia, S., and Banfić, H. (2001). Presence and activation of nuclear phosphoinositide 3-kinase C2β during compensatory liver growth. *J. Biol. Chem.* **276,** 17754–17761.

Sonzogni, L., Silvestri, L., De Silvestri, A., Gritti, C., Foti, L., Zavaglia, C., Botelli, R., Mondelli, M. U., Civardi, E., and Silini, E. M. (2002). Polymorphisms of microsomal epoxide hydrolase gene and severity of HCV-related liver disease. *Hepatology* **36,** 195–201.

Takanashi, M., and Saito, T. (2006). Characterization of two 3-hydroxybutyrate dehydrogenases in poly(3-hydroxybutyrate)-degradable bacterium, *Ralstonia pickettii* T1. *J. Biosci. Bioeng.* **101,** 501–507.

Tanaka, M., Tanaka, T., Harata, M., Suzuki, T., and Mitsui, Y. (1998). Triplet repeat-containing ribosomal protein L14 gene in immortalized human endothelial cell line (t-HUE4). *Biochem. Biophys. Res. Commun.* **243,** 531–537.

Timsit, Y. E., and Negishi, M. (2007). CAR and PXR: The xenobiotic-sensing receptors. *Steroids* **72,** 231–246.

Tsao, C., Foley, J., Coulter, S. J., Maronpot, R., Zeldin, D. C., and Goldstein, J. A. (2000). CYP2C40, a unique arachidonic acid 16-hydroxylase, is the major CYP2C in the murine intestinal tract. *Mol. Pharmacol.* **58,** 279–287.

Twigger, S. N., Shimoyama, M., Bromberg, S., Kwitek, A. E., Jacob, H. J., and the RGD Team. (2007). The Rat Genome Database, update 2007—Easing the path from disease to data and back again. *Nucleic Acids Res.* **35**(Database issue), D658–D662.

Ueda, A., Hamadeh, H. K., Webb, H. K., Yamamoto, Y., Sueyoshi, T., Afshari, C. A., Lehmann, J. M., and Negishi, M. (2002). Diverse roles of the nuclear orphan receptor CAR in regulating hepatic genes in response to phenobarbital. *Mol. Pharmacol.* **61,** 1–6.

Wang, N., Li, Z., Ding, R., Frank, G. D., Senbonmatsu, T., Landon, E. J., Inagami, T., and Zhao, Z. J. (2006). Antagonism or synergism: Role of tyrosine phosphatases *SHP-1* and *SHP-2* in growth factor signaling. *J. Biol. Chem.* **281,** 21878–21883.

Waxman, D. J., and Azaroff, L. (1992). Phenobarbital induction of cytochrome P-450 gene expression. *Biochem. J.* **281,** 577–592.

Wei, L., Imanaka-Yoshida, K., Wang, L., Zhan, S., Schneider, M. D., DeMayo, F. J., and Schwartz, R. J. (2002). Inhibition of Rho family GTPases by Rho GDP dissociation inhibitor disrupts cardiac morphogenesis and inhibits cardiomyocyte proliferation. *Development* **129,** 1705–1714.

Wellman, T. L., Jenkins, J., Penar, P. L., Tranmer, B., Zahr, R., and Lounsbury, K. M. (2004). Nitric oxide and reactive oxygen species exert opposing effects on the stability of hypoxia inducible factor-1α (HIF-1α) in explants of human pial arteries. *FASEB J.* **18,** 379–381.

Yahyaoui, W., Callejo, M., Price, G. B., and Zannis-Hadjopoulos, M. (2007). Deletion of the cruciform binding domain in CBP/14-3-3 displays reduced origin binding and initiation of DNA replication in budding yeast. *BMC Mol. Biol.* **8,** 27.

Yanbin, J., Toader, V., and Bennett, B. M. (2002). Regulation of microsomal and cytosolic glutathione S-transferase activities by S-nitrosylation. *Biochem. Pharmacol.* **63,** 1397–1404.

Yokota, S., Okabayashi, T., Yokosawa, N., and Fujii, N. (2008). Measles virus P protein suppresses Toll-like receptor signal through up-regulation of ubiquitin-modifying enzyme A20. *FASEB J.* **22,** 1–11.

Yoshida, K. (2007). PKCdelta signaling: Mechanisms of DNA damage response and apoptosis. *Cell. Signal.* **19,** 892–901.

Zgoda, V., Tikhonova, O., Viglinskaya, A., Serebriakova, M., Lisitsa, A., and Archakov, A. (2006). Proteomic profiles of induced hepatotoxicity at the subcellular level. *Proteomics* **6,** 4662–4670.